

Synthesis and biodistribution of an ^{18}F -labelled resveratrol derivative for small animal positron emission tomography

S. Gester, F. Wuest, B. Pawelke, R. Bergmann, and J. Pietzsch

Positron Emission Tomography Center, Institute of Bioinorganic and Radiopharmaceutical Chemistry,
Research Center Rossendorf, Dresden, Germany

Received December 5, 2004

Accepted February 7, 2005

Published online July 8, 2005; © Springer-Verlag 2005

Summary. Resveratrol (3,4',5-trihydroxy-*trans*-stilbene) is a naturally occurring phytoalexin and polyphenol existing in grapes and various other plants, and one of the best known 'nutriceuticals'. It shows a multiplicity of beneficial biological effects, particularly, by attenuating atherogenic, inflammatory, and carcinogenic processes. However, despite convincing evidence from experimental and clinical studies, data concerning the role of resveratrol and other members of the large polyphenols family for human health is still a matter of debate. One reason for this is the lack of suitable sensitive and specific methods, which would allow direct assessment of biodistribution, biokinetics, and the metabolic fate of these compounds *in vivo*. The unique features of positron emission tomography (PET) as a non-invasive *in vivo* imaging methodology in combination with suitable PET radiotracers have great promise to assess quantitative information on physiological effects of polyphenols *in vivo*. Herein we describe the radiosynthesis of an ^{18}F -labelled resveratrol derivative, 3,5-dihydroxy-4'- ^{18}F fluoro-*trans*-stilbene ($[^{18}\text{F}]\text{-I}$), using the Horner-Wadsworth-Emmons reaction as a novel radiolabelling technique in PET radiochemistry for subsequent functional imaging of polyphenol metabolism *in vivo*. In a typical "three-step/one-pot" reaction, ^{18}F -labelled resveratrol derivative $[^{18}\text{F}]\text{-I}$ could be synthesized within 120–130 min including HPLC separation at a specific radioactivity of about 90 GBq/ μmol . The radiochemical yield was about 9% (decay-corrected) related to $[^{18}\text{F}]\text{fluoride}$ and the radiochemical purity exceeded 97%. First radiopharmacological evaluation included measurement of biodistribution *ex vivo* and positron emission tomography (PET) studies *in vivo* after intravenous application of $[^{18}\text{F}]\text{-I}$ in male Wistar rats using a dedicated small animal PET camera with very high spatial resolution. Concordantly with data on bioavailability and metabolism of native resveratrol from the literature, these investigations revealed an extensive uptake and metabolism in the liver and kidney, respectively, of $[^{18}\text{F}]\text{-I}$. This study represents the first investigation of polyphenols *in vivo* by means of PET.

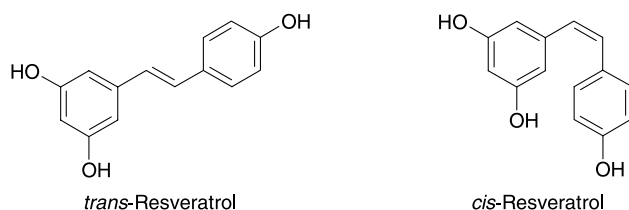
Keywords: Polyphenols – Resveratrol – $[^{18}\text{F}]\text{Fluorobenzaldehyde}$ – Horner-Wadsworth-Emmons reaction – Positron emission tomography (PET)

1 Introduction

It has been well accepted that the type of diet has an influence on human health and longevity. In this context,

much attention has been paid to several phytochemicals like polyphenols that are highly abundant food micronutrients. Polyphenols comprise a large category of more than 8000 compounds including flavonoids (the largest group), phenolic acids, coumarins, and stilbenes. Various polyphenols present in human diet show protecting effects against several diseases such as cardiovascular and neurodegenerative pathologies, diabetes mellitus, inflammation, or cancer. The polyphenol family is a rather large group of compounds, which are difficult to generalize in terms of their benefits for human health. However, it is safe to say that most of dietary polyphenols are strong antioxidants. In this way they provide protection against oxidative attack by free radicals and/or reactive oxygen (nitrogen) species, which can damage cells and tissues. Moreover, these processes are thought to be linked to the development of several chronic diseases and the aging process (Middleton et al., 2000; Kinghorn et al., 2004).

One dietary compound under intensive investigation is the stilbene resveratrol (3,4',5-trihydroxy-*trans*-stilbene). Resveratrol occurs naturally in grapevine plants and a variety of medicinal plants such as *Polygonaceae*. In these plants, resveratrol functions as a phytoalexin that protects against injury, and *Botrytis* infection and other fungal infection (Hain et al., 1990; Kimura, 2003). Resveratrol is present in *cis*- and *trans*-isomers (Scheme 1) and the major abundant *trans*-isomer is the biologically active one. Because of its high concentration in grape skin, considerable amounts of resveratrol (5–40 μM) are present in wine (Fremont, 2000). Amounts of resveratrol in red wines are significantly higher than in white wines. In this



Scheme 1. The *cis*- and *trans*-isoforms of resveratrol. The biologically active and therefore the more significant substance of both isomers is *trans*-resveratrol

context, epidemiologic studies have revealed a reduced incidence of cardiovascular risk associated with regular consume of red wine. This phenomenon has been popularized as the *French paradox* (Miller and Rice-Evans, 1995; Kopp, 1998; Bavaresco et al., 1999). In the past decade, *in vivo*, *ex vivo*, and animal experiments have shown that resveratrol possesses many biological attributes that favor protection against atherosclerosis, including inhibition of low density lipoprotein (LDL) lipid and apolipoprotein oxidation, inhibition of platelet aggregation, modulation of hepatic apolipoprotein and lipid synthesis, modulation of vasorelaxation, and inhibition of synthesis of pro-atherogenic eicosanoids by human platelets and neutrophils. Furthermore, it can reduce ischemic damage in heart ischemia/reperfusion injury and also in brain ischemia/reperfusion as shown in rodent models (Soleas et al., 1997; Wu et al., 2001; Brito et al., 2002; Kimura, 2003; Hao and He, 2004). Moreover, resveratrol has been reported to have cancer chemopreventive activity in assays representing all three major stages of carcinogenesis (Jang et al., 1997; Kundu and Surh, 2004). Because of its intrinsic radical scavenger properties, resveratrol may suppress tumor development through the removal of reactive oxygen species. Furthermore, its ability to inhibit cellular events associated with tumor initiation, promotion, and progression has been attributed to the modulation of many key proteins and enzymes in cell life by resveratrol, such as cyclooxygenases, lipoxygenase, protein kinases, ribonucleotide reductase, and P450 (Middleton et al., 2000; Haider et al., 2003; Granados-Soto, 2003; Jannin et al., 2004; Pozo-Guisado et al., 2004; Kundu and Surh, 2004). Resveratrol has been found to modulate phase II drug-metabolizing enzymes and to induce human promyelocytic leukemia cell differentiation and apoptosis. In addition, it has been found to inhibit the development of preneoplastic lesions in carcinogen-treated mouse mammary glands in culture and to inhibit tumorigenesis in a mouse skin cancer model (Jang et al., 1997). Moreover, some reports have shown that resveratrol can prevent

tumor growth and metastasis also in human lung carcinoma, pancreatic cancer, prostate cancer, and bronchial epithelioma cancer models (Yu et al., 2003). Resveratrol modulates expression and activity of inducible NO synthase (iNOS) and inducible cyclooxygenase-2 (COX-2) (Tsai et al., 1999; Cho et al., 2002). Furthermore, resveratrol has been found to possess potent protein kinase inhibitory activity, and thus exerting further modulating effects on intracellular signal transduction in the processes of cell proliferation and differentiation (Kim et al., 2003; Slater et al., 2003; Gusman et al., 2001).

Data from the literature exhibit a multiplicity of interesting properties of the polyphenol family as 'nutriceuticals' that justify further investigations on their bioavailability and their metabolic fate *in vivo* to better understand the potential link between the ingestion of these substances as dietary agents, the access to proposed cellular sites of action, and the effects of health promotion or health risk. However, also keeping in mind the large number of polyphenols, metabolic data are scarce and often controversial.

For resveratrol intestinal absorption has been demonstrated in human intestinal Caco-2 cell model and in rat small intestine model *in vitro* (Andlauer et al., 2000; Kuhnle et al., 2000; Kaldas et al., 2002; Li et al., 2003). First *in vivo* metabolic studies in mice using ^{14}C -*trans*-resveratrol showed *i)* that ^{14}C -*trans*-resveratrol is bioavailable following oral administration and remains mostly in intact form, *ii)* that ^{14}C -*trans*-resveratrol derived radioactivity is able to penetrate the tissues of liver and kidney, and *iii)* the presence of intact ^{14}C -*trans*-resveratrol together with conjugated resveratrol (glucurono- and/or sulfoconjugates) in these tissues (Vitrac et al., 2003). These findings partly confirmed some former data obtained in human volunteers (de Santi et al., 2000a; de Santi et al., 2000b). In contrast, by examining the absorption, bioavailability, and metabolism of ^{14}C -*trans*-resveratrol after oral and intravenous application in mice, rats, and in human volunteers only trace amounts of non-metabolized ^{14}C -*trans*-resveratrol could be detected in serum by other groups (Yu et al., 2002; Walle et al., 2004). In the rat, of note, it has been indicated that resveratrol may be reasonably well absorbed, although bioavailability may be low (Juan et al., 2002). In these studies, most of the oral dose was recovered in urine and LC/MS analysis identified two major metabolic pathways: sulfate and glucuronic acid conjugation of the phenolic groups (Yu et al., 2002; Walle et al., 2004). In addition, hydrogenation of the double bond could be found by Walle and colleagues (Walle et al., 2004). But the latter is likely to be produced by the intestinal microflora (Walle et al., 2004). Various

studies showed that in mice, rats, and humans extremely rapid sulfate conjugation by intestine and liver appears to be the rate-limiting step in the bioavailability of resveratrol (de Santi et al., 2000a; Yu et al., 2002; Walle et al., 2004). These studies might have implications regarding the significance of *in vitro* studies that used only non-conjugated resveratrol on further metabolites formation, e.g., hydroxylation products like piceatannol and 3,4,5,4'-tetrahydroxystilbene (Piver et al., 2004).

Despite convincing evidence from these studies, data concerning the bioavailability and metabolic fate of resveratrol and other polyphenols *in vivo* are still a matter of debate (Gescher and Steward, 2003). Studies based on ^{14}C -radiolabelled compounds, however, share certain limitations. First of all, it is difficult to obtain total recovery of the radioactivity from the whole organism. Also kinetic measurements cause some experimental expenditure when β^- -emitting nuclides are used. In such experiments it is necessary to extract and dissolve a large number of samples of the tissues studied.

Alternatively, radiolabelling with short-lived positron emitters such as ^{11}C ($t_{1/2} = 20.4$ min) and ^{18}F ($t_{1/2} = 109.8$ min) and the use of small animal positron emission tomography (PET) represents a promising approach for imaging and quantitative assessment of metabolic sites of several polyphenols non-invasively *in vivo* (Pietzsch et al., 2003). PET allows the measurement of the radioactivity distribution time profile and the radioactivity concentration in the living organism without tissue destruction or without being influenced by the composition of the tissues studied.

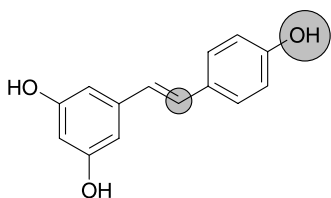
The aim of this pioneering study, therefore, was to make use of the PET modality to perform radiopharmacological studies of polyphenol derivatives *in vivo*. From both, the nutritional and physiological point of view, resveratrol was chosen as a first candidate for labelling with PET radionuclides. Considering the stilbene structure of the target molecule in combination with the special challenges for incorporation of β^+ -emitting radionuclides

into small molecules of biological relevance (Wuest, this issue), basically two different synthesis strategies can be envisaged to label resveratrol with the most prominent short-lived positron emitters ^{11}C and ^{18}F at different labelling positions (Scheme 2).

The first approach comprises isotopic labelling with ^{11}C resulting in a radiotracer, indistinguishable from the native compound. Occurring very small kinetic isotopic effects can generally be neglected. Such isotopic labelling could be achieved by exploiting a Heck reaction of a [β - ^{11}C]styrene derivative with an iodoarene. The ^{11}C -labelled styrene derivative is easily accessible either by the reaction of [^{11}C]methyltriphenylphosphonium iodide with a benzaldehyde (Kihlberg et al., 1990) or by means of a Wittig carbonyl olefination reaction between a ^{11}C -labelled benzaldehyde with methyltriphenylphosphonium salts (Björkman and Langström, 2000). Feasibility of a radiosynthesis involving short-lived positron emitters is mainly governed by the synthesis time, which should not exceed three half lives of the radionuclide, being 60 min in the case of ^{11}C . The complexity and the fairly time-consuming synthesis route involving a Wittig reaction, however, may limit the use of the proposed synthesis strategy when ^{11}C is used as the radiolabel for our first labelling attempts of polyphenols with short-lived positron emitters. Moreover, application of Wittig carbonyl olefination reaction conditions have the drawback of leading to the formation of both the desired and biologically active *trans*- and the undesired *cis*-isomer, which have to be separated in an additional purification step.

In contrast, the convenient half-life of the positron emitter ^{18}F makes this radioisotope ideally suited for radiolabelling and radiopharmacological studies. It can be produced in high quantities using a dedicated small biomedical cyclotron as the most frequently used production source. Corresponding ^{18}F -labelled radiotracers can be shipped from the production site to the imaging site, and imaging protocols can be expanded to up to 6 hours, which also permits dynamic assessment of fairly slow metabolic processes. Furthermore, ^{18}F is considered the ideal radioisotope for PET imaging owing to its low positron energy (0.64 MeV), which not only limits the dose rate when used in human studies but also results in a relatively short range of emission in tissue, thereby providing high-resolution images.

A further important assumption behind ^{18}F -labellings is the fact that the lack of a positron-emitting isotope of hydrogen can be compensated in many cases by using ^{18}F as a bioisosteric replacement for a hydrogen atom in a molecule. A fluorine atom may also imitate a hydroxyl



Scheme 2. Potential places in the *trans*-resveratrol molecule for labelling with the PET-nuclides ^{18}F or ^{11}C . The hydroxyl group offers a place for bioisosteric substitution with the nuclide ^{18}F , an isotopic labelling with ^{11}C could be achieved at the carbon indicated by the smaller circle

group. Moreover, many novel drugs contain a fluorine atom, which also can isotopically be replaced with ^{18}F (Park et al., 2001).

In this line, a second synthesis route for labelling resveratrol with a short-lived positron emitter consists of the bioisosteric replacement of one of the phenolic hydroxyl groups present in resveratrol with ^{18}F . This can be accomplished by means of a carbonyl olefination with 4- ^{18}F fluorobenzaldehyde as readily available labelling precursor. Wittig reactions of aldehydes with 4- ^{18}F fluorobenzaldehyde have been reported in the literature (Piarraud et al., 1993). However, selectivity problems regarding to the formation of *trans*- and *cis*-isomers in course of the reaction have also been observed. Thus, stable ylides preferentially result in the formation of the thermodynamically stable *trans*-isomer, whereas less stable ylides lead to the corresponding *cis*-isomer. Ylides containing aryl substituents are considered to be semi-stable and, thus, forming mixtures of both isomers. In order to circumvent the *trans*-/*cis*-selectivity problems we made use of an alternative carbonyl olefination reaction, being the Horner-Wadsworth-Emmons reaction. This novel radiolabelling technique in ^{18}F chemistry is capable of creating a carbon-carbon double bond, which exclusively displays the desired *trans*-isomer configuration as found in the stilbene scaffold of resveratrol. Thus, by coupling phosphonic acid diester **4c** with readily available 4- ^{18}F fluorobenzaldehyde (^{18}F -**5**) and subsequent cleavage of the MOM-protecting groups would lead to resveratrol derivative ^{18}F -**1** displaying the desired *trans*-configuration.

Furthermore, preliminary radiopharmacological evaluation by means of biodistribution and small animal PET imaging studies in male Wistar rats after intravenous application of ^{18}F -**1** was performed. As a major finding, these investigations revealed an extensive uptake and metabolism of ^{18}F -**1** in the liver and kidney, respectively. This approach may be expected to find many uses in studies investigating the mechanisms and potential health effects of flavonoids.

2 Materials and methods

General procedures

All reactions were performed under nitrogen atmosphere with oven-dried glassware. Tetrahydrofuran was distilled from sodium/benzophenone prior to use. 4-trimethylammonium-benzaldehyde triflate (4-formyl- N^i , N^i , N^i -trimethyl-1-benzenaminium trifluoromethanesulfonate; **7**) was synthesized according to Wilson and colleagues (Wilson et al., 1990). All other starting materials and reagents were obtained commercially and used without further purification. Analytical thin-layer chromatography was

carried out on Merck silica gel F-254 plates with UV-visualization. Flash chromatography was performed using Merck silica gel (230–400 mesh) according to Still and colleagues (Still et al., 1978). ^1H -NMR spectra were recorded on a Varian Inova-400 at 400 MHz. Chemical shifts are determined relative to the solvent and converted to the TMS scale.

Chemical syntheses

Methyl 3,5-bis(methoxymethoxy)benzoate; **3**

To a stirred solution of the phenol **2** (1.00 g, 5.95 mmol) in THF (30 mL) was added DIPEA (2.31 g, 17.9 mmol) and MOMCl (1.44 g, 17.9 mmol). The mixture was stirred at reflux overnight and another portion of DIPEA (0.77 g, 5.95 mmol) and MOMCl (0.48 g, 5.95 mmol) was added. After end of reaction (monitored by thin layer chromatography) water (65 mL) was added. The mixture was extracted with CH_2Cl_2 (3 \times 50 mL), washed with brine (50 mL), water (50 mL) and dried over Na_2SO_4 . Filtration and solvent evaporation gave protected MOM-ether **3** as colorless oil, which was used without further purification. Yield: 1.55 g (>99%). R_f = 0.50 (ethyl acetate/petrol ether 50/50). ^1H -NMR (CDCl_3), δ 3.48 (s, 6H, $-\text{OCH}_2\text{OCH}_3$), 3.90 (s, 3H, $-\text{CO}_2\text{CH}_3$), 5.19 (s, 4H, $-\text{OCH}_2\text{OCH}_3$), 6.91 (t, 1H, 4J = 2.2 Hz, Ar-H), 7.37 (d, 2H, 4J = 2.2 Hz, Ar-H).

[3,5-bis(Methoxymethoxy)phenyl]methanol; **4a**

To a cooled (0°C) solution of LiAlH_4 (4.8 mL 1 M in Et_2O , 4.8 mmol) in Et_2O (8 mL) was added the MOM-ether **3** (1.00 g, 3.90 mmol) in Et_2O (15 mL) while stirring. The reaction mixture was warmed up to room temperature and stirring was continued for 1 h. After carefully quenching with water (30 mL), the mixture was extracted with CH_2Cl_2 (1 \times 30 mL, 3 \times 15 mL). The combined organic layers were washed with brine (30 mL) and dried over Na_2SO_4 . Solvent evaporation gave the alcohol **4a** as colorless oil, which was used for the following reaction without purification. Yield: 817 mg (92%). R_f = 0.28 (ethyl acetate/petrol ether 50/50). ^1H -NMR (CDCl_3), δ 1.73 (s, br, 1H, $-\text{CH}_2\text{OH}$), 3.47 (s, 6H, $-\text{OCH}_2\text{OCH}_3$), 4.63 (s, 2H, $-\text{CH}_2\text{OH}$), 5.16 (s, 4H, $-\text{OCH}_2\text{OCH}_3$), 6.65 (t, 1H, 4J = 2.2 Hz, Ar-H), 6.72 (d, 2H, 4J = 2.2 Hz, Ar-H).

1-(Bromomethyl)-3,5-bis(methoxymethoxy)benzene; **4b**

To a stirred solution of the alcohol **4a** (2.28 g, 10.0 mmol) and PPh_3 (5.24 g, 20.0 mmol) in DMF (25 mL) was added *N*-bromosuccinimide (NBS) (3.56 g, 20.0 mmol) in portions. The reaction mixture was warmed up to 60°C and stirring was continued for 1 h. After quenching with water (100 mL), the mixture was extracted with Et_2O (3 \times 50 mL) and CH_2Cl_2 (2 \times 50 mL). The combined organic layers were dried over Na_2SO_4 and the solvent was evaporated. The residue was purified by flash chromatography (ethyl acetate/petrol ether 50/50) to give bromide **4b** as an oil. Yield: 1.62 g (56%). R_f = 0.58 (ethyl acetate/petrol ether 50/50). ^1H -NMR (CDCl_3), δ 3.48 (s, 6H, $-\text{OCH}_2\text{OCH}_3$), 4.41 (s, 2H, $-\text{CH}_2\text{Br}$), 5.16 (s, 4H, $-\text{OCH}_2\text{OCH}_3$), 6.67 (t, 1H, 4J = 2.2 Hz, Ar-H), 6.74 (d, 2H, 4J = 2.2 Hz, Ar-H).

Diethyl [3,5-bis(methoxymethoxy)benzyl]phosphonate; **4c**

A stirred mixture of bromide **4b** (1.62 g, 5.57 mmol) and triethyl phosphite (1.85 g, 11.1 mmol) was heated to 160°C for 3 h. The reaction mixture was cooled down to room temperature and purified by flash chromatography (100% ethyl acetate) to give phosphonic acid diester **4c** as a pale yellow oil. Yield: 1.27 g (65%). R_f = 0.25 (100% ethyl acetate). ^1H -NMR (CDCl_3), δ 1.27 (t, 6H, $\text{PO}(\text{OCH}_2\text{CH}_3)_2$), 3.06 (s, 1H, $-\text{CH}_2-\text{PO}(\text{OEt})_2$), 3.11 (s, 1H, $-\text{CH}_2-\text{PO}(\text{OEt})_2$), 3.46 (s, 6H, $-\text{OCH}_2\text{OCH}_3$), 4.04 (q, 4H, $\text{PO}(\text{OCH}_2\text{CH}_3)_2$), 5.14 (s, 4H, $-\text{OCH}_2\text{OCH}_3$), 6.62 (t, 1H, 4J = 2.2 Hz, Ar-H), 6.65 (d, 2H, 4J = 2.2 Hz, Ar-H).

1-[(*E*)-2-(4-Fluorophenyl)ethenyl]-
3,5-bis(methoxymethoxy)benzene; **6**

To a stirred solution of phosphonic acid diester **4c** (50 mg, 0.144 mmol) and 4-fluorobenzaldehyde **5** (18 mg, 0.144 mmol) in 1.2 mL DMF was added KO^tBu (41 mg, 0.364 mmol) in 1.2 mL DMF. Stirring was continued at room temperature for 1 h. The reaction mixture was poured into crushed ice and extracted with CH_2Cl_2 (2×10 mL). The combined organic layers were dried over Na_2SO_4 and the solvent was evaporated. The residue was purified by flash chromatography (ethyl acetate/petrol ether 50/50) to give fluorostilbene **6** as a colorless oil. Yield: 46 mg (>99%). $R_f = 0.66$ (ethyl acetate/petrol ether 50/50). $^1\text{H-NMR}$ (CDCl_3), δ 3.51 (s, 6H, $-\text{OCH}_2\text{OCH}_3$), 5.20 (s, 4H, $-\text{OCH}_2\text{OCH}_3$), 6.67 (t, 1H, $^4J = 2.2$ Hz, Ar-H), 6.86 (d, 2H, $^4J = 2.2$ Hz, Ar-H), 6.94 (AB quartet, $\Delta\nu = 39.0$ Hz, 1H, $J = 16.1$ Hz, Ar-CH=CH-ArF), 7.04 (AB quartet, $\Delta\nu = 39.0$ Hz, 1H, $J = 16.1$ Hz, Ar-CH=CH-ArF), 7.04–7.46 (m, 4H, Ar-H).

5-[(*E*)-2-(4-Fluorophenyl)ethenyl]-1,3-benzenediol; **1**

To a stirred solution of fluorostilbene **6** (46 mg, 0.144 mmol) in MeOH (3.0 mL) was added 3M HCl (0.2 mL). Stirring was continued at room temperature for 30 min. Then saturated NaHCO_3 (2 mL) was added to the reaction mixture and MeOH was evaporated. After extracting the reaction mixture with ethyl acetate (3×5 mL) the combined organic layers were dried over Na_2SO_4 , filtered and the solvent was evaporated. The crude product was purified by flash chromatography (ethyl acetate/petrol ether 50/50) to give *trans*-fluorostilbene **1** (*trans*-/*cis*-ratio >95%, determined by $^1\text{H-NMR}$ spectroscopy) as colorless crystals. Yield: 31 mg (93%). $R_f = 0.32$ (ethyl acetate/petrol ether 50/50). $^1\text{H-NMR}$ (CDCl_3), δ 4.76 (s, 2H, Ar-OH), 6.28 (t, 1H, $^4J = 2.2$ Hz, Ar-H), 6.56 (d, 2H, $^4J = 2.2$ Hz, Ar-H), 6.87 (AB quartet, $\Delta\nu = 52.1$ Hz, 1H, $J = 16.1$ Hz, Ar-CH=CH-ArF), 7.00 (AB quartet, $\Delta\nu = 52.1$ Hz, 1H, $J = 16.1$ Hz, Ar-CH=CH-ArF), 7.05–7.45 (m, 4H, Ar-H).

Radiochemical syntheses

5-[(*E*)-2-(4- ^{18}F Fluorophenyl)ethenyl]-1,3-benzenediol; [^{18}F]-**1**

No-carrier-added aqueous [^{18}F]fluoride was produced in an IBA CYCLONE 18/9 cyclotron by irradiation of [^{18}O]H $_2\text{O}$ via the $^{18}\text{O}(\text{p},\text{n})^{18}\text{F}$ nuclear reaction. Resolubilization of the aqueous [^{18}F]fluoride was accomplished with Kryptofix $^{\text{®}}$ 2.2.2 and K_2CO_3 in

an automated nucleophilic fluorination module (Nuclear Interface, Münster). 4- ^{18}F fluorobenzaldehyde [^{18}F]-**5** was synthesized according to Maeding and Steinbach (Maeding and Steinbach, 2002) starting from 4-trimethylammonium-benzaldehyde triflate **7**.

HPLC analyses were carried out with a Supelco Supelcosil $^{\text{TM}}$ LC-18S column (250×4.6 mm, $5 \mu\text{m}$) using an isocratic eluent ($\text{CH}_3\text{CN}/0.1$ M ammonium formate) at a flow rate of 1 mL/min. The products were monitored by an UV detector L4500 (Merck, Hitachi) at 250 nm and by γ -detection with a scintillation detector GABI Star (X-Raytest). Semi-preparative HPLC was performed with a Hamilton PRP $^{\text{®}}$ -1 column (250×10 mm, $10 \mu\text{m}$) using isocratic elution with $\text{CH}_3\text{CN}/0.1$ M ammonium formate (50/50) at a flow rate of 3 mL/min. For radio-TLC detection a BAS 2000 scanner (Fujix) was used. Cyclotron produced [^{18}F]HF (8 GBq) was dried in a remotely-controlled fluorination module according to Roemer and coworkers (Roemer et al., 2001).

Then, 4-trimethylammonium-benzaldehyde triflate **7** (15 mg, 47.9 μmol) dissolved in DMF (1 mL) was added and the reaction mixture was heated at 120°C for 15 min. After cooling the reaction vessel to 60°C , phosphonate precursor **4c** (10 mg, 28.7 μmol) and KO^tBu (8 mg, 71.3 μmol) dissolved in DMF (2 mL) were added to the reaction mixture. The coupling-reaction was carried out for 15 min. Then 3M HCl (2 mL) was added to remove the MOM-protecting groups. After 20 min, the mixture was diluted with H $_2\text{O}$ (10 mL) and passed through a LiChrolut RP18 cartridge (500 mg). The cartridge was washed with water (5 mL) and the product mixture was eluted from the cartridge with acetonitrile (3 mL) and subjected onto a semi-preparative HPLC column. The fraction eluting at 18.0 min was collected, diluted with water (25 mL) and passed through a Macherey-Nagel Chromafix $^{\text{®}}$ C18ec cartridge. The cartridge was washed with water (5 mL) and the product was finally eluted from this cartridge with 1 mL of EtOH. This “three-step/one-pot” procedure provides radiochemical and chemical pure 5-[(*E*)-2-(4- ^{18}F fluorophenyl)ethenyl]-1,3-benzenediol ([^{18}F]-**1**). Radiochemical yield: 330 MBq (9% decay-corrected, related to [^{18}F]fluoride). The radiochemical purity of the product is greater than 95% (Fig. 1). The specific activity was determined to be about 90 GBq/ μmol .

Radiopharmacological characterization

Incubation of [^{18}F]-**1** with HepG $_2$ cells

HepG $_2$ cells, a human hepatocyte carcinoma cell line, were obtained from the European Collection of Cell Cultures (ECACC; Salisbury, England). Cells were grown in RPMI 1640 medium supplemented with 10% (v/v)

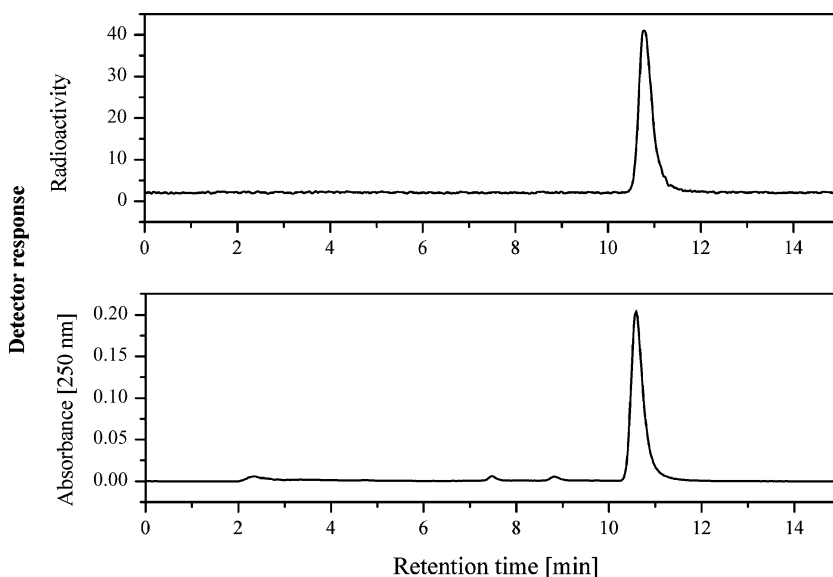


Fig. 1. HPLC analysis of carrier added [^{18}F]-**1** with radioactivity and UV absorbance detection showing radiochemical purity of [^{18}F]-**1** >95%

fetal calf serum (FCS), penicillin (100 U/mL), streptomycin (100 µg/mL), and glutamine (2 mM) at 37°C and 5% CO₂ in a humidified incubator. For the cell incubation studies, cells were seeded in 24-well plates at a density of 1×10^5 cells/mL. Twenty-four hours later, cells were incubated for 30 min at 4°C and at 37°C, respectively, with [^{18}F]-**1** (0.3 MBq per well; radiochemical purity 92%; medium) in a total volume of 250 µL. At the appropriate time point, plates were removed from the incubator and cell supernatant was removed. Remaining cells were rinsed twice with 1 mL of PBS containing 0.1% (w/v) bovine serum albumin, then twice with 1 mL of PBS. Then, the cells were harvested and lysed. Supernatants and cell lysates were counted for radioactivity (Cobra II gamma counter, Canberra-Packard, Meriden, CT, USA), deproteinated with the twofold volume of ethanol, and then subjected to analysis of radioactive metabolites by HPLC as described elsewhere in this issue (Pawelke, 2005). The HPLC system (HP1100, Agilent Technologies, Waldbronn, Germany) was equipped with a guard-column (ZORBAX 300SB-C18, 4.6 × 12.5 mm, 5 µm), a semi-preparative column (ZORBAX 300SB-C18, 9.4 × 250 mm, 5 µm), a variable-wavelength UV detector and a radiochromatography detector (Canberra-Packard, Meriden, CT, USA). Typically, 50–200 µL (10–20 kBq) of supernatant or cell lysate samples were injected and compounds were separated using gradient conditions at 40°C and a flow rate of 2 mL/min. Solvent A comprised of acetonitrile with 0.04% TFA, solvent B comprised of water with 0.05% TFA. The gradient steps were: 0–10 min 20% to 100% A, 10–12 min 100% A, 12–13.5 min to 20% A. For UV-detection the wavelength of 214 nm was used. The reference compound [^{18}F]-**1** eluted on this system with a retention time of 11.9 min (Pawelke, 2005).

Animal experiments

All animal experiments were carried out with male Wistar rats (aged 6 weeks; 160–170 g) according to the guidelines of the German Regulations for Animal Welfare. The protocol was approved by the local Ethical Committee for Animal Experiments. Animals were kept under a 12 h light-dark cycle and fed with commercial animal diet and water ad libitum. For biodistribution studies, the animals were injected with approximately 1.5 MBq [^{18}F]-**1** (radiochemical purity 97%) in 0.5 mL saline with 2% ethanol into the tail vein under light ether anaesthesia. After injection animals in groups of four rats were sacrificed by heart puncture under ether anaesthesia at 5 and 60 min, respectively. Organs and tissues of interest were rapidly excised, weighed, and the radioactivity was determined (Cobra II gamma counter, Canberra-Packard, Meriden, CT, USA). The accumulated radioactivity in organs and tissues was calculated as the percentage of the injected dose localised per gram tissue (%ID/g tissue). For each animal, radioactivity of the tissue samples was calibrated against a known aliquot of injectate. Values are expressed as mean ± standard deviation (SD) for a group of four animals.

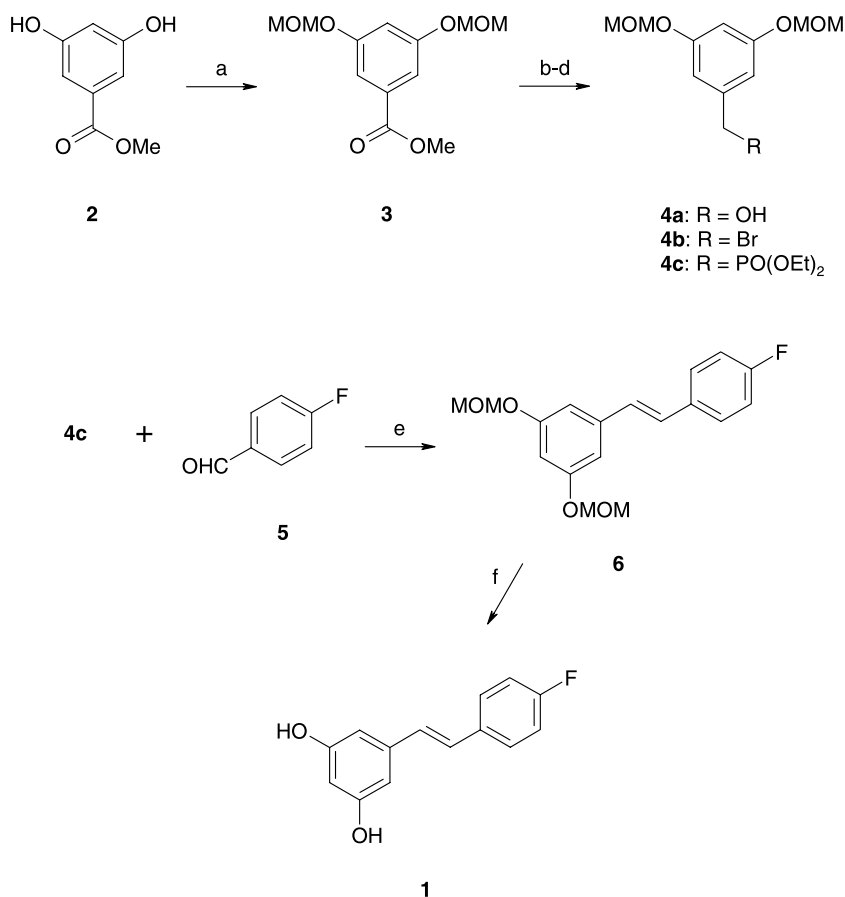
For metabolite analysis, animals were anesthetized with urethane (1.3 g/kg body weight) and catheters were placed into both the right external jugular vein and the right common carotid artery. A volume of 0.5 mL of [^{18}F]-**1** (10–20 MBq, radiochemical purity 92–97%) in saline with 2% ethanol was injected in the vein. At 5 and 55 min after injection blood samples (0.3 mL) were taken from the arteria. The depleted blood volume was compensated for by injection of saline. 60 min after injection the animals were sacrificed by heart puncture under light ether anaesthesia and urine samples were taken (0.5 mL). Blood and urine samples were centrifuged at room temperature (11.000 × g for 3 min). Both plasma and urine samples were deproteinated with the twofold volume of ethanol. The plasma and urine samples were analysed by HPLC as described above.

As an adjunct, dynamic PET studies were performed with a dedicated PET scanner for small animals (microPET P4, CTI Concorde Microsystems, Knoxville, TN, USA) as published elsewhere (Pietzsch et al., 2005). In brief, the scanner has a field-of-view (FOV) of 8 cm axially by 22 cm transaxially and operates in 3-dimensional list mode. The raw data were sorted into three-dimensional sinogram data and converted to

two-dimensional format by Fourier rebinning (FORE). Iterative image reconstruction was performed using two-dimensional ordered subsets expectation maximization (OSEM) using the microPET P4 software package. Image reconstruction was carried out with attenuation correction. Corrections were applied for variability in line of response detection efficiency (normalization) and random coincidences. The spatial resolution obtained ranged from 2.2 to 2.3 mm. No correction for recovery and partial volume effects was applied. For imaging studies, animals were anesthetized with urethane (1.3 g/kg body weight) and catheters were placed into the right external jugular vein or, alternatively, into the femoral vein. The animals under urethane anesthesia were then positioned and immobilized supine with their medial axis parallel to the axial axis of the scanner with thorax and abdominal region (organs of interest: heart, liver, kidneys, intestine, bladder) in the center of FOV. For the purpose of photon attenuation correction, a transmission scan was carried out before tracer administration. The radiotracers were then administered as a 0.5 mL bolus (approximately 10 MBq of [^{18}F]-**1**) via the catheters within 15 seconds. Simultaneously with tracer injection, dynamic PET scanning was started for 60 min using the following time intervals (frames) for sinogram generation: 12 × 10 s, 6 × 30 s, 5 × 300 s, and 3 × 600 s. Time-activity-curves (TAC) representing the total ^{18}F -radioactivity concentration in a defined volume were obtained from the small animal PET images in each rat by defining separate 3-dimensional regions-of-interest (ROI) for the heart region (representing the cardiac blood pool), the liver, the kidneys, and the intestine by the ROIFinder software package developed by Poetzsch and colleagues (Poetzsch et al., 2003). TACs are given as radioactivity concentration, percent of maximum.

3 Results

Starting from commercially available methyl 3,5-dihydroxybenzoate **2** the phenolic hydroxyl groups were protected in quantitative yield by reaction with MOMCl under basic conditions using DIPEA in a standard procedure. The obtained MOM-ether **3** was converted into [3,5-bis(methoxymethoxy)phenyl]methanol **4a** via reduction with LiAlH₄ in Et₂O in 92% yield according to Sun and coworkers (Sun et al., 1998). Following the procedure by Wuest and colleagues (Wuest et al., 2004), subsequent bromination of benzylic alcohol **4a** with NBS/PPh₃ in DMF gave bromide **4b** in 56% yield. 1-(Bromomethyl)-3,5-bis(methoxymethoxy)benzene **4b** was converted into diethyl [3,5-bis(methoxymethoxy)-benzyl]phosphonate **4c** employing Michaelis-Arbuzov reaction conditions according to Meier and Dullweber (Meier and Dullweber, 1997). In this way labelling precursor **4c** could be obtained in 65% yield. Coupling of the phosphonic acid diester **4c** with 4-fluorobenzaldehyde **5** under Horner-Wadsworth-Emmons conditions (KO^tBu, DMF, see Gerold et al., 2001) leads to the formation of pure 1-[(*E*)-2-(4-fluorophenyl)ethenyl]-3,5-bis(methoxymethoxy)benzene **6** in quantitative yield (a conventional Wittig synthesis with the ylen/yliid-analogue of compound **4c** would provide a mixture of the *trans*- and *cis*-isomers (Pettit et al., 2002)). Removal of MOM-protecting groups in **6** was accomplished by treatment with diluted HCl in MeOH at room

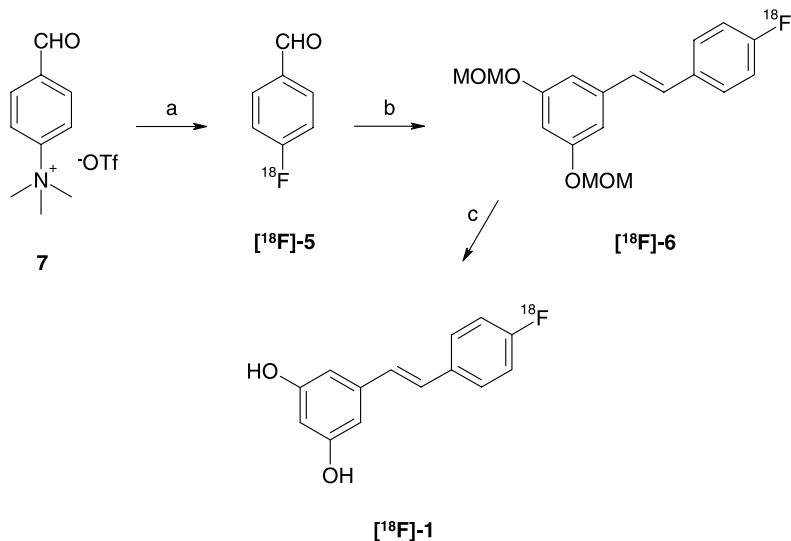


Scheme 3. Synthesis of reference compound **1** and radiolabelling precursor **4c**. Reagents and conditions: (a) MOMCl, DIPEA, THF, reflux, >99%; (b) LiAlH₄, Et₂O, 0°C-RT, 92%; (c) NBS, PPh₃, DMF, 60°C, 56%; (d) P(OEt)₃, 160°C, 65%; (e) KO^tBu, DMF, >99%; (f) MeOH, HCl, 93%

temperature according to Germain and Deslongchamps (Germain and Deslongchamps, 2002) (Scheme 3). In this way, resveratrol derivative 5-[(*E*)-2-(4-fluorophenyl)ethenyl]-1,3-benzenediol **1** was isolated in 93% yield with an *trans*–/*cis*-ratio greater than 95% as determined by ^1H -

NMR spectroscopy. ^1H -NMR analytical data correspond well with data from the literature (Morita et al., 2001).

Radiolabelling was performed using the readily available 4- ^{18}F fluorobenzaldehyde [^{18}F]-**5** as coupling partner in course of a Horner-Wadsworth-Emmons reaction



Scheme 4. “Three step/one pot” synthesis of [^{18}F]-**1**. Reagents and conditions: (a) [^{18}F] F^- , K₂CO₃/Kryptofix₂₂₂, DMF, 120°C, 15 min; (b) **4c**, KO^tBu, DMF, 60°C, 15 min; (c) 3M HCl, 60°C, 20 min

with phosphonic acid diester **4c**. 4- ^{18}F Fluorobenzaldehyde was synthesized according to Maeding and Steinbach (Maeding and Steinbach, 2002) starting from 4-trimethylammonium-benzaldehyde triflate **7** as the labelling precursor (Wilson et al., 1990) and ^{18}F fluoride/Kryptofix[®] 2.2.2 in DMF as the solvent. After cooling, a solution of phosphonic acid diester **4c** and potassium tert.-butoxide as the base in DMF was added to the crude reaction mixture containing 4- ^{18}F fluorobenzaldehyde [^{18}F]-**5**. The resulting ^{18}F fluorine labelled coupling product 1-[(*E*)-2-(4- ^{18}F fluorophenyl)ethenyl]-3,5-bis(methoxymethoxy)benzene [^{18}F]-**6** was treated with 3 M HCl to remove the MOM-protecting groups to give 5-[(*E*)-2-(4- ^{18}F fluorophenyl)ethenyl]-1,3-benzenediol [^{18}F]-**1** in a “three-step/one-pot” reaction sequence (Scheme 4).

The analyzed ^1H -NMR data of **1** show a coupling constant of 16.1 Hz indicative of the olefinic protons, as typical found for *trans*-isomers and resulting from the mechanism of the Horner-Wadsworth-Emmons reaction. By employing a similar carbonyl olefination protocol as exemplified for the synthesis of compound **1** we also expect formation of the *trans*-isomer of the radiofluorinated resveratrol derivative [^{18}F]-**1**. This assumption was proved by comparison of the HPLC profile of reference compound **1** with radiolabelled compound [^{18}F]-**1** ($t_R = 10.8$ min, $\text{CH}_3\text{CN}/0.1$ M ammonium formate 40/60, 1 mL/min).

The decay-corrected radiochemical yield of [^{18}F]-**1** was 9% after HPLC-purification. The specific activity reaches up to 90 GBq/ μmol , and the radiochemical purity exceeded 95% as determined by radio-HPLC (Fig. 1).

Furthermore, we performed first experiments aiming at the biological behavior of [^{18}F]-**1** *in vitro* and *in vivo*. Table 1 shows the distribution of ^{18}F -radioactivity in male Wistar rats after a single intravenous injection of [^{18}F]-**1**. Data were obtained at 5 and 60 min post injection. The biodistribution studies showed a very rapid clearance of ^{18}F -radioactivity from the blood compartment. The radioactivity concentration at 5 min was nearly on the final level (0.15 ± 0.02 %ID/g). This process was accompanied by a rapid uptake both in the liver and the kidneys. The fast systemic clearance was similarly accompanied by hepatobiliary and renal elimination. In the urine were 28.8 ± 5.1 and 37.9 ± 5.2 percent of injected dose (%ID) at 5 and 60 min, respectively. In the intestine were 4.8 ± 0.8 and 31.1 ± 3.0 %ID at 5 and 60 min, respectively. The low accumulation of radioactivity in the femoral bone after 5 min and 60 min, respectively, is indicative of a low *in vivo* defluorination of [^{18}F]-**1**. The observed ^{18}F -radioactivity organ concentration in the rat after intravenous administration of [^{18}F]-**1** reflects the predominant non-specific distribution according the expected high lipophilicity of the compound (for comparison, log K_W of *trans*-

Table 1. Radioactivity, expressed as percent injected dose (%ID) and percent injected dose per gram tissue (%ID/g), in different organs after single intravenous injection of 1.5 MBq [^{18}F]-**1** in 0.5 mL saline with 2% ethanol

Organ	%ID		%ID/g	
	5 min p.i.	60 min p.i.	5 min p.i.	60 min p.i.
Blood	0.92 ± 0.37	0.31 ± 0.12	0.53 ± 0.09	0.15 ± 0.02
Brown fat	0.17 ± 0.05	0.03 ± 0.01	0.45 ± 0.08	0.06 ± 0.01
Brain	0.58 ± 0.20	0.07 ± 0.02	0.33 ± 0.12	0.05 ± 0.01
Pancreas	0.30 ± 0.07	0.06 ± 0.01	0.52 ± 0.11	0.09 ± 0.01
Spleen	0.44 ± 0.12	0.32 ± 0.10	0.72 ± 0.15	0.48 ± 0.19
Adrenals	0.06 ± 0.01	0.02 ± 0.00	0.86 ± 0.23	0.22 ± 0.02
Kidney	9.50 ± 0.35	5.59 ± 1.23	4.86 ± 1.09	2.71 ± 0.54
White fat	0.05 ± 0.01	0.02 ± 0.01	0.16 ± 0.06	0.06 ± 0.01
Muscle	0.11 ± 0.02	0.03 ± 0.01	0.20 ± 0.01	0.04 ± 0.01
Heart	0.29 ± 0.03	0.08 ± 0.01	0.37 ± 0.10	0.10 ± 0.02
Lung	2.27 ± 0.32	0.49 ± 0.03	1.67 ± 0.37	0.34 ± 0.04
Thymus	0.17 ± 0.03	0.05 ± 0.01	0.30 ± 0.14	0.07 ± 0.02
Thyroid gland	0.05 ± 0.02	0.02 ± 0.00	0.43 ± 0.09	0.13 ± 0.02
Harder glands	0.09 ± 0.01	0.02 ± 0.00	0.38 ± 0.13	0.08 ± 0.01
Liver	25.26 ± 3.29	12.59 ± 1.11	2.18 ± 0.55	1.03 ± 0.24
Femur	0.19 ± 0.02	0.05 ± 0.01	0.18 ± 0.04	0.05 ± 0.00
Testes	0.17 ± 0.02	0.09 ± 0.01	0.07 ± 0.01	0.03 ± 0.01
Intestine	4.79 ± 0.84	31.05 ± 3.00	–	–
Urine	28.81 ± 5.13	37.87 ± 5.15	–	–

Results are means \pm SD (n = 4)

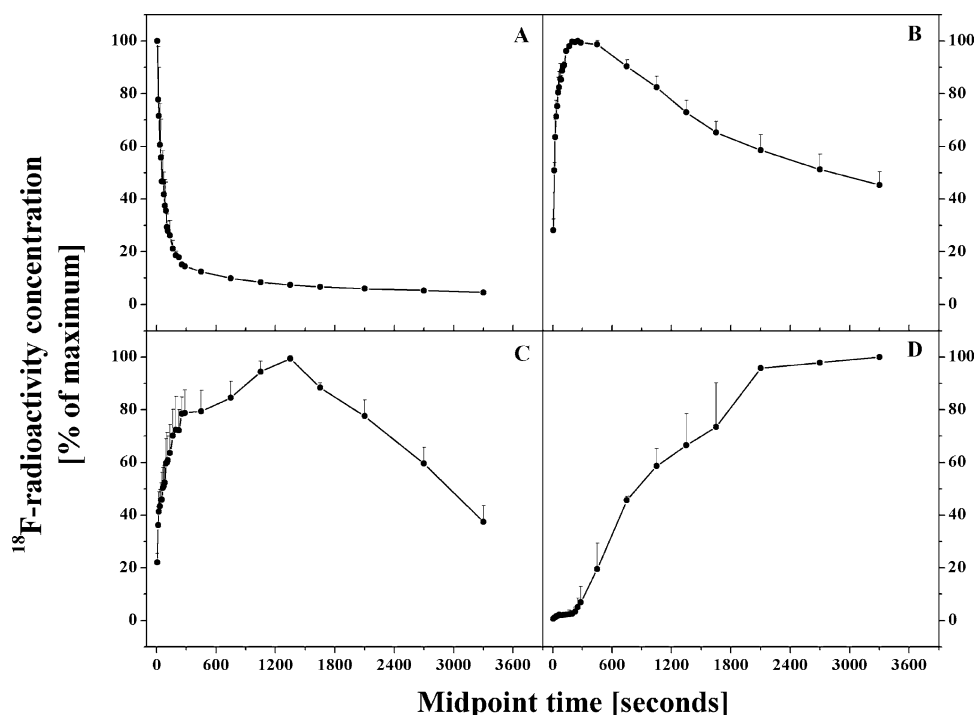


Fig. 2. Kinetics of the ^{18}F -radioactivity calculated by PET measurements from ROIs (regions of interest) over the heart (A), the liver (B), the kidney (C), and the intestine (D). Results are expressed as means \pm SD of three independent experiments

resveratrol equals to 2.03 as determined by Varache-Lembège and colleagues (Varache-Lembège et al., 2000), and is consistent with data from the literature. These data could be confirmed by small animal PET imaging studies. From these studies, time-activity-curves were obtained for the heart (majorly representing the cardiac blood pool), the liver, the kidneys, and the intestine (Figs. 2 and 3). The results from ROI analysis of these organs, showing fast blood clearance, rapid uptake in liver and kidney, and substantial excretion of ^{18}F -radioactivity into the intestine, agreed well with the corresponding results obtained from biodistribution experiments. The tissue localization of ^{18}F -radioactivity reflecting both $[^{18}\text{F}]\text{-I}$ and its labelled metabolites, as well as very fast excretion of ^{18}F -radioactivity into bile/intestine and urine is consistent with findings on rapid formation of hydrophilic metabolites from resveratrol and analogues in the literature. In order to develop a first approach to the study of metabolism of ^{18}F -labelled resveratrol derivatives *in vitro* and, to understand the relation between the measured radioactivity concentrations in blood, intestine, and urine obtained from biodistribution and small animal PET studies *in vivo*, we undertook the determination of radioactive species as potential metabolites of *n.c.a.* $[^{18}\text{F}]\text{-I}$ in several biological specimen by HPLC (Pawelke, 2005). The original tracer compound $[^{18}\text{F}]\text{-I}$ and at least two radioactive metabo-

lites observed were well separated under the chromatographic conditions employed, with their retention times ($[^{18}\text{F}]\text{-I}$, 11.9 min; metabolite Mb1, 10.5 min; and metabolite Mb2, 10.2 min) being very reproducible. Furthermore, dependent on its radiochemical purity (ranging from 92–97%) the original tracer compound contained one minor impurity (no radioactivity signal intensity greater than 5%). This impurity could be recovered at a retention time of 12.5 min in both cellular and plasma samples, but not in urine and in intestine, respectively. For the performed cellular experiments and the animal studies in rats, we essentially expected that, similar to *trans*-resveratrol, $[^{18}\text{F}]\text{-I}$ undergoes metabolic transformation to its 3-glucurono- and/or 3-sulfoconjugates, but not to its 4'-glucurono- and/or 4'-sulfoconjugates due to substitution of ^{18}F for the hydroxyl group at position 4'. As a result, after incubation of $[^{18}\text{F}]\text{-I}$ with HepG₂ cells for 30 min, $[^{18}\text{F}]\text{-I}$ showed significant metabolization with one major radioactive metabolite, Mb1, observed in cell lysates to a low extent of 11% of total ^{18}F -radioactivity at 4°C and to a higher extent of 59% at 37°C, respectively. Similarly, the corresponding supernatants contained excreted Mb1 to a low extent of 4% of total ^{18}F -radioactivity at 4°C and to a higher extent of 29% at 37°C, respectively. Thus, formation of Mb1 reflects the activity of a certain metabolic process in HepG₂ cells *in vitro*.

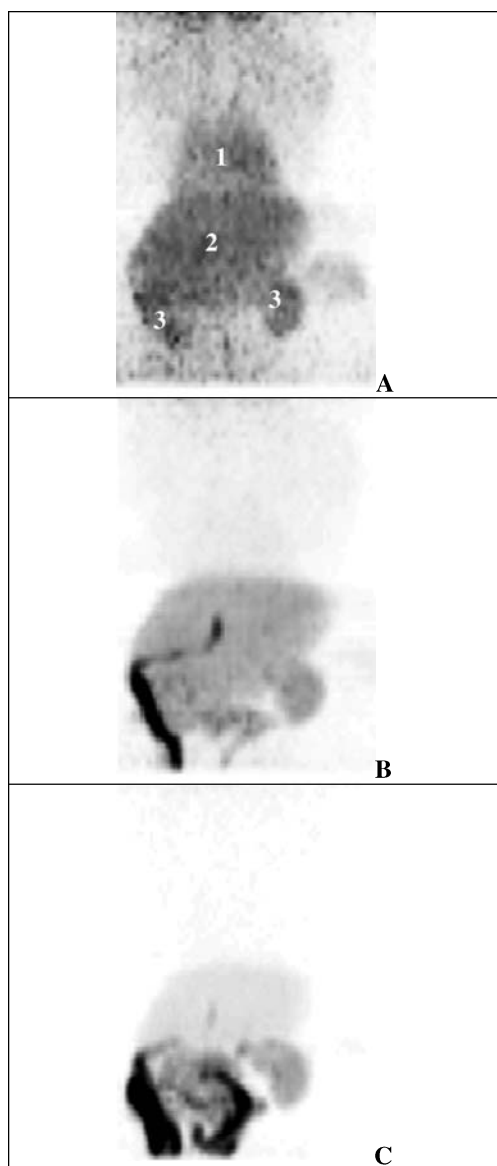


Fig. 3. Representative coronal small animal PET images (thoracic and abdominal region, maximum intensity projection) showing distribution of ^{18}F -radioactivity at 2 min (A), 30 min (B), and 60 min (C) after intravenous injection of $[^{18}\text{F}]\text{-I}$ in the rat. Numbers in (A) indicate the cardiac region (1), the liver (2), and the kidneys (3). (B) and (C) illustrate hepatobiliary excretion and intestinal passage of ^{18}F -radioactivity

Plasma samples of male Wistar rats obtained at 5 and 55 min after intravenous administration of $[^{18}\text{F}]\text{-I}$ also revealed very fast metabolism *in vivo*. After 5 min $[^{18}\text{F}]\text{-I}$ was nearly completely cleared from plasma. More than 70% of total plasma radioactivity could be attributed to two major metabolites, Mb1 (32% of total ^{18}F -radioactivity) and, to a higher extent, a more hydrophilic compound Mb2 (41% of total ^{18}F -radioactivity). After 55 min in plasma only traces of Mb1 and Mb2 but no $[^{18}\text{F}]\text{-I}$ still could be detected. In *ex vivo* urine samples 60 min after

intravenous administration of $[^{18}\text{F}]\text{-I}$ more than 65% of total radioactivity could be attributed to Mb1 (32% of total ^{18}F -radioactivity) and Mb2 (50% of total ^{18}F -radioactivity). Furthermore, in *ex vivo* intestinal samples 60 min after intravenous administration of $[^{18}\text{F}]\text{-I}$ more than 70% of total radioactivity could be attributed to Mb1 (47% of total ^{18}F -radioactivity) and Mb2 (26% of total ^{18}F -radioactivity), respectively. In contrast to plasma and urine samples, in intestine Mb1 showed a higher abundance than Mb2.

4 Discussion

For the first time a representative compound of the polyphenol substance class could successfully be labelled with a short-lived positron emitter, being ^{18}F -labelled resveratrol derivative $[^{18}\text{F}]\text{-I}$, which was subjected to preliminary radiopharmacological characterization.

As an important food micronutrient resveratrol was chosen as a first candidate for radiolabelling with a positron emitter by bioisosteric replacement of the hydroxyl group in the 4'-position with readily available positron emitter ^{18}F . Subsequent preliminary radiopharmacological investigations involving biodistribution and *in vivo* PET-studies revealed first insights on pharmacokinetics of ^{18}F -labelled $[^{18}\text{F}]\text{-I}$ as radiolabelled surrogate of the polyphenol resveratrol as compound with potential relevance and importance for food sciences. The key step to build up the stilbene scaffold of the resveratrol derivative $[^{18}\text{F}]\text{-I}$ consists of a carbonyl olefination reaction with the readily available labelling precursor 4- $[^{18}\text{F}]$ fluorobenzaldehyde $[^{18}\text{F}]\text{-5}$. To date, carbon-carbon bond forming reactions created by a Wittig type of reaction are not well explored in ^{18}F -chemistry. First results revealed substantial *trans*- and *cis*-isomer selectivity problems. Thus, dependent on the stability of the *in situ* generated ylides different ratios of *trans*- and *cis*-isomers as well as the formation of by-products could be observed as reported by Piarraud and coworkers (Piarraud et al., 1993). Therefore, we set up an alternative synthesis route involving a Horner-Wadsworth-Emmons reaction as the key step to enable exclusive formation of the *trans*-isomer of ^{18}F -labelled resveratrol derivative $[^{18}\text{F}]\text{-I}$. This method represents a valuable novel labelling technique in ^{18}F -chemistry. As a stereoselective operating carbon-carbon bond forming reaction this procedure provides a general approach for the formation of ^{18}F -labelled stilbene-like compounds exclusively displaying *trans*-configuration. 4- $[^{18}\text{F}]$ fluorobenzaldehyde $[^{18}\text{F}]\text{-5}$, the coupling partner in the Horner-Wadsworth-Emmons reaction with phosphonic acid diester **4c**, represents a

well known and readily available ^{18}F -labelling precursor. Compound $[^{18}\text{F}]\text{-5}$ can be synthesized starting from 4-trimethylammonium-benzaldehyde triflate **7** in high radiochemical yields (Maeding and Steinbach, 2002). Moreover, 4- $[^{18}\text{F}]$ fluorobenzaldehyde $[^{18}\text{F}]\text{-5}$ can be used without laborious purification steps, which facilitates automation of the entire radiosynthesis of resveratrol derivative $[^{18}\text{F}]\text{-1}$. Hence, the radiosynthesis of the ^{18}F -labelled resveratrol derivative $[^{18}\text{F}]\text{-1}$ could be carried out completely in a remotely controlled synthesis apparatus. Automation permits safe handling of even high amounts of radioactivity through significant reduction of radiation exposure to the personnel. Besides the important reduction of radiation exposure to personnel, automation is also an inevitable necessity to meet regulatory compliances, namely good manufacturing practice (GMP) and good laboratory practice (GLP) guidelines. Therefore, remotely controlled automation of radiochemical syntheses is highly desirable to enable a widespread use of PET.

The “three-step/one-pot”-reaction of $[^{18}\text{F}]\text{-1}$ succeeded in radiochemical yields of 9% (decay-corrected) after semi-preparative HPLC-purification at high specific radioactivity (about 90 GBq/ μmol) and high radiochemical purity (>95%). The found high specific radioactivity of 90 GBq/ μmol is in the range usually required for specific binding radiotracers. Automation of the radiosynthesis allows handling of large amounts of $[^{18}\text{F}]$ fluoride as starting material to afford resveratrol derivative $[^{18}\text{F}]\text{-1}$ in sufficient quantities and quality necessary for subsequent radiopharmacological investigations.

Biodistribution and small animal PET imaging studies showed ^{18}F -radioactivity after intravenous administration of $[^{18}\text{F}]\text{-1}$ to be very rapidly cleared from the blood compartment, completely due to high levels of uptake in liver and kidney, followed by substantial hepatobiliary and renal excretion. Of note, in the present study all cellular and animal experiments have been performed with *n.c.a.* $[^{18}\text{F}]\text{-1}$ representing picomolar amounts of the tracer and its expected metabolites. In this context, it has to be considered, that the ^{18}F -radioactivity only at the moment of injection represents $[^{18}\text{F}]\text{-1}$. Due to metabolism different metabolic species carrying ^{18}F can be formed in the course of time. For obtaining quantitative data on metabolism of labelled resveratrol and other polyphenols these metabolites have to be identified and metabolite-specific ^{18}F -radioactivity has to be determined thus allowing further analyses. However, this study revealed very fast metabolism of $[^{18}\text{F}]\text{-1}$. Experiments using human hepatocyte carcinoma cells (HepG₂) showed rapid uptake and metabolism of $[^{18}\text{F}]\text{-1}$. The metabolite Mb1 reflects the activity

of certain metabolic processes in HepG₂ *in vitro* and of the liver *in vivo*. A comparison of chromatographic characteristics of the cell metabolites and of those excreted from the body in urine and the intestine showed a second abundant metabolite (Mb2) only occurring in the living animal. For comparison, the biotransformation of resveratrol in humans and laboratory animals has been described (Walle et al., 2004; Yu et al., 2002; Meng et al., 2004). In general, the doses of resveratrol have been higher in animals than in humans. As in humans, the bioavailability after oral or intravenous application seems to be low and the metabolism involves formation of majorily resveratrol 3-*O*- and 4'-*O*-glucuronides and -sulfates, respectively (Yu et al., 2002; Meng et al., 2004; Walle et al., 2004). In the rat, intestinal and liver glucuronidation of resveratrol is of major importance, with a small contribution of sulfation (Kuhnle et al., 2000; Juan et al., 2002). In contrast, in humans sulfate conjugation by the intestine/liver appears to be the rate-limiting step in resveratrol's bioavailability (Walle et al., 2004). When given orally, in humans a third pathway due to hydrogenation of the aliphatic double bond of the molecule has been described (Walle et al., 2004). The latter is likely produced by the intestinal microflora. Data from studies also using human hepatocytes showed glucuronidation to be the major biotransformation pathway in these cells (Yu et al., 2002). In sharp contrast to these findings, in human intestinal cell line Caco-2 mainly sulfation and, to a minor extent, glucuronidation was involved in resveratrol metabolism (Kaldas et al., 2003). Considering the substitution of the 4'-OH group for by ^{18}F , in the case of $[^{18}\text{F}]\text{-1}$ only formation of its 3-*O*-glucuronides and -sulfates essentially could be expected (Walle, 2004). This is consistent with the present study. Having in mind the intrinsic problems of quantitative analysis and identification of metabolites when tracers were applied under *n.c.a.* conditions, in this pioneering study only an estimation of radioactivity distribution has been initially performed (Pawelke, 2005). From the present data and the literature it can be assumed that Mb1 represents a glucuronide and Mb2 represents a sulfate of $[^{18}\text{F}]\text{-1}$, respectively, however, the identity of these metabolites has to be confirmed by further investigations (Yu et al., 2002; Walle, 2004).

Diet-derived polyphenols, such as resveratrol, with interesting cancer chemopreventive properties in experimental models, remain attractive as clinical candidates. One reason for their attractiveness is the fact that the long-proven use of their dietary sources suggests low potential for unwanted side effects, although this notion may not hold if they are administered at high doses as

single agents (Gescher and Steward, 2003). Although many studies have implicated a role for resveratrol and other polyphenols in disease prevention, information on *in vivo* bioavailability and metabolism of these compounds is largely incomplete, thus the benefits of these compounds as chemopreventive dietary or dietary supplemental agents are still only "potential". This preliminary study aimed at the development of a new methodology to implement the PET modality in investigations on biological behavior of resveratrol and other polyphenols.

Further research on the radiolabelling of polyphenols with short-lived positron emitters should be directed to an isotopic labelling of *trans*-resveratrol with ^{11}C as PET radiotracer. Possible synthetic routes to ^{11}C -labelled resveratrol should make use of the novel elaborated radiolabelling approach involving a Horner-Wadsworth-Emmons reaction. In the case of ^{11}C -labelled resveratrol the reaction should preferentially occur between a phosphonic acid ester and an appropriate ^{11}C -labelled benzaldehyde to give the stilbene derivative in the desired *trans*-configuration. An alternative approach would comprise a Heck reaction between a ^{11}C -labelled styrene derivative and an arylhalide. Despite the inherent difficulties encountered during complex radiolabelling reactions with the short-lived positron emitter ^{11}C , both approaches would provide a ^{11}C -labelled resveratrol indistinguishable from its native counterpart. This fact would allow radiopharmacological studies, which will reflect metabolic pathways of natural resveratrol.

In summary, in this work we have described for the first time the radiosynthesis of a polyphenol as relevant for food sciences labelled with a short-lived positron emitter along with preliminary radiopharmacological investigations by means of PET. The radiosynthesis of resveratrol derivative [^{18}F]-**1** is based on a bioisosteric replacement of a phenolic hydroxyl group of resveratrol with the positron emitter ^{18}F . The radiosynthesis was accomplished via a carbonyl olefination reaction with 4-[^{18}F]fluorobenzaldehyde as the key step in the reaction sequence. Moreover, such a Horner-Wadsworth-Emmons reaction with readily available 4-[^{18}F]fluorobenzaldehyde represents a novel approach for distinct C–C double bond formations in ^{18}F chemistry yielding exclusively stilbene derivatives with *trans*-configuration.

Biodistribution and microPET experiments showed that the resulting compound [^{18}F]-**1** or related compounds could prove to be suitable *in vivo* probes for the metabolic fate of resveratrol and other polyphenols. As a limitation, in the present study the novel tracer compound was administered only intravenously and, with respect to the bio-

availability as one major question of interest in food sciences, does not reflect its ingestion, intestinal absorption, and access to intended sites of action. Furthermore, metabolic conversions which take place in the intestine have not been accounted. However, this study provides additional evidence that metabolites of resveratrol and not its free form is found to predominate in the circulation. The latter suggests that the potential biologic activity of resveratrol metabolites, such as glucuronide and sulfate conjugates, should be considered in future experimental and clinical investigation. In this context, it also remains to be elucidated whether accumulation of potentially active resveratrol metabolites in epithelial cells along the digestive tract may still produce cancer preventive and other effects (Walle et al., 2004). Corresponding studies are currently in progress.

Acknowledgements

The authors are very grateful to Mareike Barth, Regina Herrlich, Heidmarie Kasper, Tilow Krauss, Stephan Preusche, and Katrin Rode for their excellent technical assistance.

References

- Andlauer W, Kolb J, Siebert K, Furst P (2000) Assessment of resveratrol bioavailability in the perfused small intestine of the rat. *Drugs Exp Clin Res* 26: 47–55
- Bavaresco L, Fregoni C, Cantu E, Trevisan M (1999) Stilbene compounds: from the grapevine to wine. *Drugs Exp Clin Res* 25: 57–63
- Bergmann R, Helling R, Heichert C, Scheunemann M, Maeding P, Wittrisch H, Johannsen B, Henle T (2001) Radio fluorination and positron emission tomography (PET) as a new approach to study the *in vivo* distribution and elimination of the advanced glycation endproducts N epsilon-carboxymethyllysine (CML) and N epsilon-carboxyethyllysine (CEL). *Food* 45: 182–188
- Björkman M, Langström B (2000) Functionalisation of ^{11}C -labelled alkenes via a Heck coupling reaction. *J Chem Soc Perkin Trans 1* 2000: 3031–3034
- Brito P, Almeida LM, Dinis TC (2002) The interaction of resveratrol with ferrylmyoglobin and peroxynitrite; protection against LDL oxidation. *Free Radic Res* 36: 621–631
- Cho DI, Koo NY, Chung WJ, Kim TS, Ryu SY, Im SY, Kim KM (2002) Effects of resveratrol-related hydroxystilbenes on the nitric oxide production in macrophage cells: structural requirements and mechanism of action. *Life Sci* 71: 2071–2082
- De Santi C, Pietrabissa A, Spisni R, Mosca F, Pacifici GM (2000a) Sulphation of resveratrol, a natural product present in grapes and wine, in the human liver and duodenum. *Xenobiotica* 30: 609–617
- De Santi C, Pietrabissa A, Mosca F, Pacifici GM (2000b) Glucuronidation of resveratrol, a natural product present in grape and wine, in the human liver. *Xenobiotica* 30: 1047–1054
- Fremont L (2000) Biological effects of resveratrol. *Life Sci* 66: 663–673
- Germain J, Deslongchamps P (2002) Total synthesis of (±)-Momilactone A. *J Org Chem* 67: 5269–5278
- Gerold J, Holzenkamp U, Meier H (2001) Bis-, Tris-, and Tetrakis (squaraines) linked by stilbenoid scaffolds. *Eur J Org Chem* 14: 2757–2763

- Gescher AJ, Steward WP (2003) Relationship between mechanisms, bioavailability, and preclinical chemopreventive efficacy of resveratrol: a conundrum. *Cancer Epidemiol Biomarkers Prev* 12: 953–957
- Granados-Soto V (2003) Pleiotropic effects of resveratrol. *Drug News Perspect* 16: 299–307
- Gusman J, Malonne H, Atassi G (2001) A reappraisal of the potential chemopreventive and chemotherapeutic properties of resveratrol. *Carcinogenesis* 22: 1111–1117
- Haider UG, Sorescu D, Griendling KK, Vollmar AM, Dirsch VM (2003) Resveratrol increases serine15-phosphorylated but transcriptionally impaired p53 and induces a reversible DNA replication block in serum-activated vascular smooth muscle cells. *Mol Pharmacol* 63: 925–932
- Hain R, Bieseler B, Kindl H, Schroder G, Stocker R (1990) Expression of a stilbene synthase gene in *Nicotiana tabacum* results in synthesis of the phytoalexin resveratrol. *Plant Mol Biol* 15: 325–335
- Hao HD, He LR (2004) Mechanisms of cardiovascular protection by resveratrol. *J Med Food* 7: 290–298
- Jang MS, Cai EN, Udeani GO, Slowing KV, Thomas CF, Beecher CWW, Fong HHS, Farnsworth NR, Kinghorn AD, Mehta RG, Moon RC, Pezzuto JM (1997) Cancer chemopreventive activity of resveratrol, a natural product derived from grapes. *Science* 275: 218–220
- Jannin B, Menzel M, Berlot J-P, Delmas D, Lançon A, Latruffe N (2004) Transport of resveratrol, a cancer chemopreventive agent, to cellular targets: plasmatic protein binding and cell uptake. *Biochem Pharmacol* 68: 1113–1118
- Juan ME, Buenafuente J, Casals I, Planas JM (2002) Plasmatic levels of trans-resveratrol in rats. *Food Res Int* 35: 195–199
- Kaldas MI, Walle UK, Walle T (2003) Resveratrol transport and metabolism by human intestinal Caco-2 cells. *J Pharm Pharmacol* 55: 307–312
- Kihlberg T, Gullberg P, Langström B (1990) [^{11}C]Methylenetriphenylphosphorane, a new ^{11}C -precursor, used in a one-pot Wittig synthesis of [β - ^{11}C]styrene. *J Labelled Compd Radiopharm* 28: 1115–1120
- Kim YA, Rhee SH, Park KY, Choi YH (2003) Antiproliferative effect of resveratrol in human prostate carcinoma cells. *J Med Food* 6: 273–280
- Kimura Y (2003) Pharmacological studies on resveratrol. *Methods Find Exp Clin Pharmacol* 25: 297–310
- Kinghorn AD, Su BN, Jang DS, Chang LC, Lee D, Gu JQ, Carcache-Blanco EJ, Pawlus AD, Lee SK, Park EJ, Cuendet M, Gills JJ, Bhat K, Park HS, Mata-Greenwood E, Song LL, Jang M, Pezzuto JM (2004) Natural inhibitors of carcinogenesis. *Planta Med* 70: 691–705
- Kopp P (1998) Resveratrol, a phytoestrogen found in red wine. A possible explanation for the conundrum of the 'French paradox'? *Eur J Endocrinol* 138: 619–620
- Kuhnle G, Spencer JP, Chowrimootoo G, Schroeter H, Debnam ES, Srai SK, Rice-Evans C, Hahn U (2000) Resveratrol is absorbed in the small intestine as resveratrol glucuronide. *Biochem Biophys Res Commun* 272: 212–217
- Kundu JK, Surh YJ (2004) Molecular basis of chemoprevention by resveratrol: NF-kappaB and AP-1 as potential targets. *Mutat Res* 555: 65–80
- Li Y, Shin YG, Yu C, Kosmeder JW, Hirschelman WH, Pezzuto JM, van Breemen RB (2003) Increasing the throughput and productivity of Caco-2 cell permeability assays using liquid chromatography-mass spectrometry: application to resveratrol absorption and metabolism. *Comb Chem High Throughput Screen* 6: 757–767
- Maeding P, Steinbach J (2002) Synthesis of 4-[^{18}F]fluorobenzaldehyde – an important labelling moiety in ^{18}F chemistry. In: Johannsen B, Seifert S (eds) *Institute of Bioinorganic and Radiopharmaceutical Chemistry: Annual Report 2001 (FZR-340)*. Research Center Rossendorf, Dresden, p 58
- Meier H, Dullweber U (1997) Extension of the squaraine chromophore in symmetrical bis(stilbenyl)squaraines. *J Org Chem* 62: 4821–4826
- Meng X, Maliakal P, Lu H, Lee MJ, Yang CS (2004) Urinary and plasma levels of resveratrol and quercetin in humans, mice, and rats after ingestion of pure compounds and grape juice. *J Agric Food Chem* 52: 935–942
- Middleton E Jr, Kandaswami C, Theoharides TC (2000) The effects of plant flavonoids on mammalian cells: implications for inflammation, heart disease, and cancer. *Pharmacol Rev* 52: 673–751
- Miller NJ, Rice-Evans CA (1995) Antioxidant activity of resveratrol in red wine. *Clin Chem* 41:1789
- Morita H, Noguchi H, Schröder J, Abe I (2001) Novel polyketides synthesized with a higher plant stilbene synthase. *Eur J Biochem* 268: 3759–3766
- Park BK, Kitteringham NR, O'Neill PM (2001) Metabolism of fluorine-containing drugs. *Annu Rev Pharmacol Toxicol* 41: 443–470
- Pawelke B (2005) Metabolite analysis in positron emission tomography studies: examples from food sciences. *Amino Acids* 29: 377–388
- Pettit GR, Grealish MP, Jung MK, Hamel E, Pettit RK, Chapuis JC, Schmidt JM (2002) Antineoplastic agents. 465. Structural modification of resveratrol: sodium resverastatin phosphate. *J Med Chem* 45: 2534–2542
- Piarraud A, Lasne MC, Barré L, Vaugeois JM, Lancelot JC (1993) Synthesis of no carrier added [^{18}F] GBR 12936 via a Wittig reaction for use in the dopamine reuptake site study. *J Labelled Compd Radiopharm* 32: 253–254
- Pietzsch J, Bergmann R, Wuest F (2003) Flavonoide – Wirkmechanismen und neue Anwendungsmöglichkeiten (Teil 2). *Bioforum* 26: 384–385
- Pietzsch J, Bergmann R, Wuest F, Pawelke B, Hultsch C, van den Hoff J (2005) Catabolism of native and oxidized low density lipoproteins: *in vivo* insights from small animal positron emission tomography studies. *Amino Acids* 29: 389–404
- Piver B, Fer M, Vitrac X, Merillon JM, Dreano Y, Berthou F, Lucas D (2004) Involvement of cytochrome P450 1A2 in the biotransformation of trans-resveratrol in human liver microsomes. *Biochem Pharmacol* 68: 773–782
- Poetzsch C, Beuthien-Baumann B, van den Hoff J (2003) Teilautomatisierte Segmentierung zur Quantifizierung von Metastasen bei der FDG-PET. *Nuklearmedizin* 42: 26
- Pozo-Guisado E, Lorenzo-Benayas MJ, Fernandez-Salguero PM (2004) Resveratrol modulates the phosphoinositide 3-kinase pathway through an estrogen receptor alpha-dependent mechanism: relevance in cell proliferation. *Int J Cancer* 109: 167–173
- Roemer J, Fuechtner F, Steinbach J, Kasch H (2001) Automated synthesis of 16 α -[^{18}F]fluoroestradiol-3,17 β -disulphamate. *Appl Radiat Isot* 55: 631–639
- Soleas GJ, Diamandis EP, Goldberg DM (1997) Wine as a biological fluid: history, production, and role in disease prevention. *J Clin Lab Anal* 11: 287–313
- Slater SJ, Seiz JL, Cook AC, Stagliano BA, Buzas CJ (2003) Inhibition of protein kinase C by resveratrol. *Biochim Biophys Acta* 1637: 59–69
- Still WC, Kahn M, Mitra A (1978) Rapid chromatographic technique for preparative separation with moderate resolution. *J Org Chem* 43: 2923–2925
- Sun WY, Zong Q, Gu RL, Pan BC (1998) Synthesis of ardisinol II. *Synthesis* 11: 1619–1622
- Tsai SH, Lin-Shiau SY, Lin JK (1999) Suppression of nitric oxide synthase and the down-regulation of the activation of NF-kappaB in macrophages by resveratrol. *Br J Pharmacol* 126: 673–680
- Varache-Lembège M, Teguo PW, Richard T, Monti JP, Deffieux G, Vercateren J, Méillon JM, Nuhrich A (2000) Structure-activity relationships of polyhydroxystilbene derivatives extracted from *Vitis vinifera* cell cultures as inhibitors of human platelet aggregation. *Med Chem Res* 10: 253–267
- Vitrac X, Desmouliere A, Brouillaud B, Krisa S, Deffieux G, Barthe N, Rosenbaum J, Merillon JM (2003) Distribution of [^{14}C]-trans-

- resveratrol, a cancer chemopreventive polyphenol, in mouse tissues after oral administration. *Life Sci* 72: 2219–2233
- Walle T (2004) Absorption and metabolism of flavonoids. *Free Radic Biol Med* 36: 829–837
- Walle T, Hsieh F, DeLegge MH, Oatis JE, Walle UK (2004) High absorption but very low bioavailability of oral resveratrol in humans. *Drug Metab Dispos* 32: 1377–1382
- Wilson AA, Dannals RF, Ravert HT, Wagner HN Jr (1990) Reductive amination of [^{18}F]fluorobenzaldehydes: radiosynthesis of [2- ^{18}F] and [4- ^{18}F]fluorodexetimides. *J Labelled Compd Radiopharm* 28: 1189–1199
- Wu JM, Wang ZR, Hsieh TC, Bruder JL, Zou JG, Huang YZ (2001) Mechanism of cardioprotection by resveratrol, a phenolic antioxidant present in red wine. *Int J Mol Med* 8: 3–17
- Wuest F (2005) Aspects of positron emission tomography radiochemistry as relevant for food chemistry. *Amino Acids* 29: 323–339
- Wuest F, Mueller M, Bergmann R (2004) Synthesis of 4-([^{18}F]fluoromethyl)-2-chlorophenylisothiocyanate: a novel bifunctional ^{18}F -labeling agent. *Radiochim Acta* 92: 349–353
- Yu C, Shin YG, Chow A, Li Y, Kosmeder JW, Lee YS, Hirschelman WH, Pezzuto JM, Mehta RG, van Breemen RB (2002) Human, rat, and mouse metabolism of resveratrol. *Pharm Res* 19: 1907–1914
- Yu L, Sun ZJ, Wu SL, Pan CE (2003) Effect of resveratrol on cell cycle proteins in murine transplantable liver cancer. *World J Gastroenterol* 9: 2341–2343
-
- Authors' address:** Frank Wuest, PhD, PET Center, Institute of Bioinorganic and Radiopharmaceutical Chemistry, Research Center Rossendorf, P.O. Box 51 01 19, 01314 Dresden, Germany,
E-mail: f.wuest@fz-rossendorf.de